Electronic Supplementary Material (ESI) for New Journal of Chemistry.

Supplementary Materials

Facile fabrication of electrospun g-C_3N_4/$Bi_{12}O_{17}Cl_2$/poly(acrylonitrile-co-maleic acid) heterojunction nanofibers for boosting visible-light catalytic ofloxacin degradation

Zhujun Huang, Dongying Zhu, Haiyan Wang, Jinhua Luo, Chenxi Zhao, Fuyou Du*

[a]College of Biological and Environmental Engineering, Changsha University, Changsha 410022, China

* Corresponding author: F. Du

Tel.: +86-731-84261506

Fax.: +86-731-84261382

E. mail: dufu2005@126.com (F. Du)

jhluo@ccsu.cn (L. Luo)

Preparation of poly(acrylonitrile-co-maleic acid)

Poly(acrylonitrile-co-maleic acid) (PANCMA) was synthesized by using in situ polymerization of acrylonitrile and maleic anhydride. Briefly, maleic anhydride (7.407 g), acrylonitrile (13.15 mL, ρ= 0.8060 g/L), and deionized water (20 mL) were poured into a three-necked flask, then the mixed solution pH was adjusted to 2.0 with dilute sulfuric acid and heated to 60 °C under magnetic stirring. After the temperature was equilibrated at 60 °C, $K_2S_2O_8$ (0.136 g) and Na_2SO_3 (0.0766 g) were added and reacted for 3 h with the protection of N_2. The resulting polymer was taken out and washed with water and ethanol for several times, respectively, and then filtered, dried at 60 °C in a vacuum oven for 12 h.

Tables

Table S1 Calibration curve, linearity, linear regression coefficient (R^2), and limit of detection (LOD) for determination of OFL by HPLC-UV method

Compound	Calibration curve	Linearity (ng/mL)	R^2	LOD (ng/mL)	RSD (%)
OFL	y=89.086x-419.16	5-1000	0.9992	2.13	1.52

Note: The limit of detection (LOD) was evaluated on the basis of a signal-to-noise ratio of 3.

Table S2 Results of N_2 adsorption-desorption characteristics on the E-spun PANCMA and g-C_3N_4/$Bi_{12}O_{17}Cl_2$/PANCMA nanofibers

Property	**Parameter**	**PANCMA**	**g-C_3N_4/ $Bi_{12}O_{17}Cl_2$/PANCMA**
Surface Area	Single point surface area at P/Po (m^2/g)	24.9760	5.3186
	BET Surface Area (m^2/g)	25.8848	5.3938
	t-Plot External Surface Area (m^2/g)	26.1887	1.6485
	BJH Adsorption cumulative surface area of pores between 1.7000 nm and 300.0000 nm diameter (m^2/g)	25.036	2.541
	BJH Desorption cumulative surface area of pores between 1.7000 nm and 300.0000 nm diameter (m^2/g)	46.0199	3.2018
Pore Volume	Single point adsorption total pore volume of pores less than 130.9985 nm diameter at P/Po=0.985000000 (cm^3/g)	0.134838	0.013393
	t-Plot micropore volume (cm^3/g)	-0.000190	0.002134
	BJH Adsorption cumulative volume of pores between 1.7000 nm and 300.0000 nm width (cm^3/g)	0.138315	0.016434
	BJH Desorption cumulative volume of pores between 1.7000 nm and 300.0000 nm diameter (cm^3/g)	0.140227	0.018148
Pore Size	Adsorption average pore width (4V/A by BET) (nm)	20.83660	9.93196
	BJH Adsorption average pore width (4V/A) (nm)	22.0990	25.8736
	BJH Desorption average pore width (nm)	12.1884	22.6716

TableS 3 Comparison of the developed g-C_3N_4/$Bi_{12}O_{17}Cl_2$/PANCMA nanofibers with the other reported photocatalytical materials for removal of OFL

Materials	Removal mode	Time (min)	Removal efficiency	Cycle times	Referencev
MoO_3/Ag/g-C_3N_4	Photocatalytic degradation	100	89%	7	[31]
UiO-67/CdS/rGO	Photocatalytic degradation	30	93.4%	4	[32]
Bi_2MoO_6-rGO-TiO_2	Photocatalytic degradation	120	92.3%	5	[33]
$BiVO_4$/g-C_3N_4/$NiFe_2O_4$	Photocatalytic degradation	20	93.8%	5	[34]
Bi_2WO_6/Fe_3O_4/biochar	Photocatalytic degradation	60	83.1%	5	[35]
ZnO/Bi_2MoO_6	Dark adsorption	30	93%	5	[36]
	Photocatalytic degradation	90			
g-C_3N_4/NH_2-MIL-88B(Fe)	Dark adsorption	30	96.5%	3	[37]
	Photocatalytic degradation	150			
UiO-66/wood composite	Dark adsorption	90	80.96%	4	[38]
	Photocatalytic degradation	270			
E-spun g-C_3N_4/$Bi_{12}O_{17}Cl_2$/PANCMA nanofibers	Dark adsorption	6	94.8%	15	This work
	Photocatalytic degradation	20			

Figure S1 The appearance of g-C_3N_4/$Bi_{12}O_{17}Cl_2$ (A), E-spun PANCMA (B) and g-C_3N_4/$Bi_{12}O_{17}Cl_2$/PANCMA (C) nanofibers

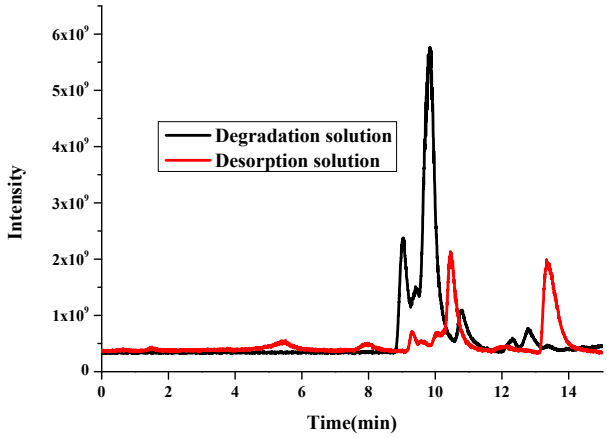

Figure S2 Typical total ion chromatograms of desorption and degradation solution by photocatalytic degradation of OFL adsorbed on E-spun g-C_3N_4/$Bi_{12}O_{17}Cl_2$(1:3)/PANCMA nanofibers

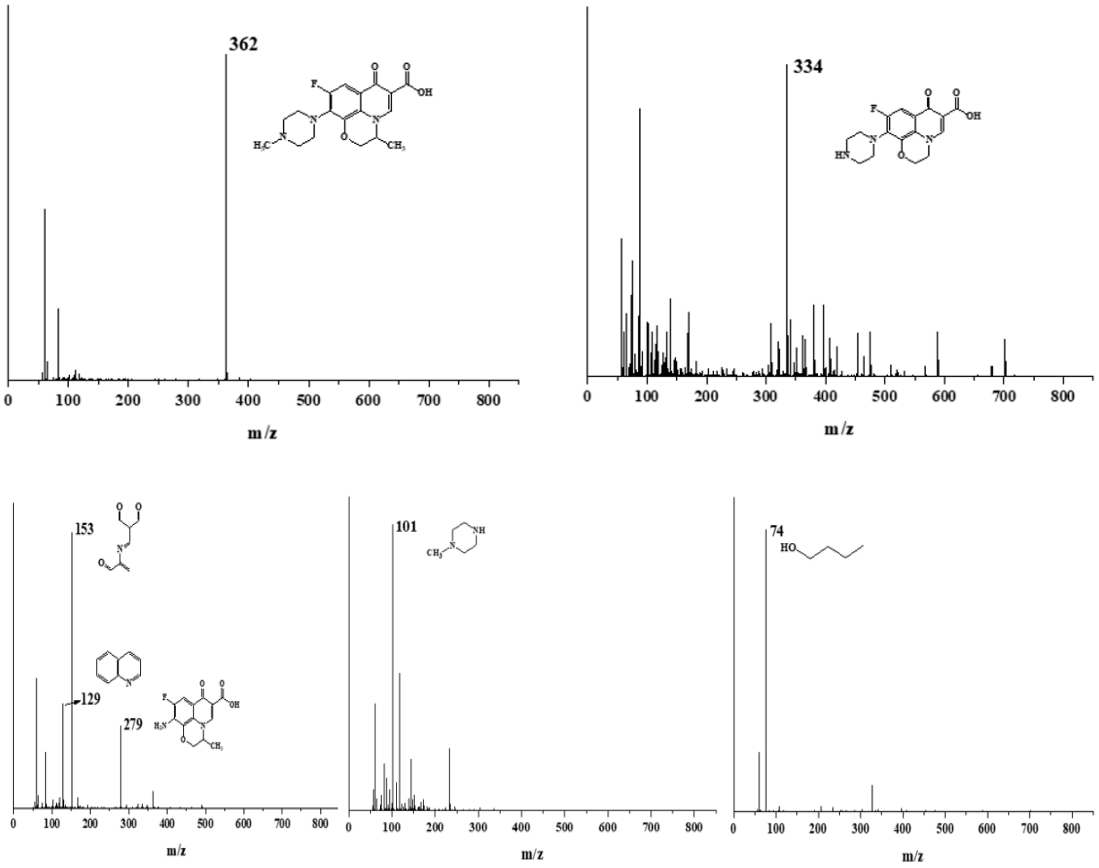

Figure S3 Typical characteristic MS fragment peaks of degradation products of OFL

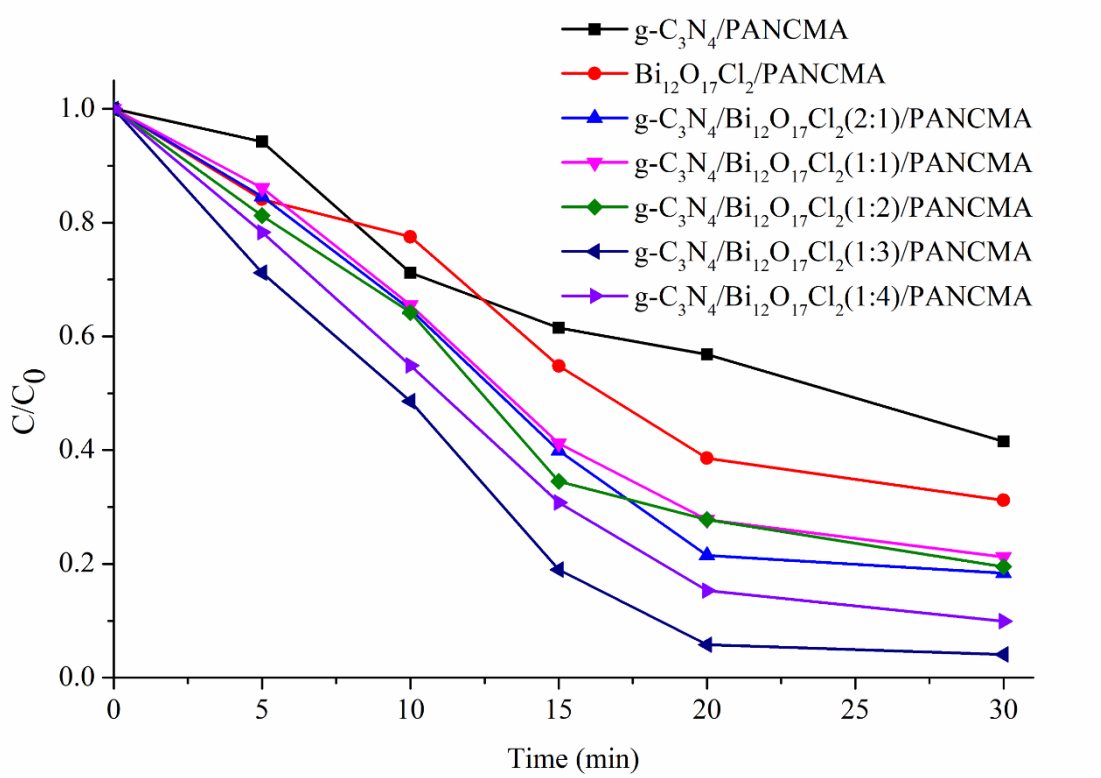

Figure S4 Effect of different photocatalytical materials on the OFL degradation

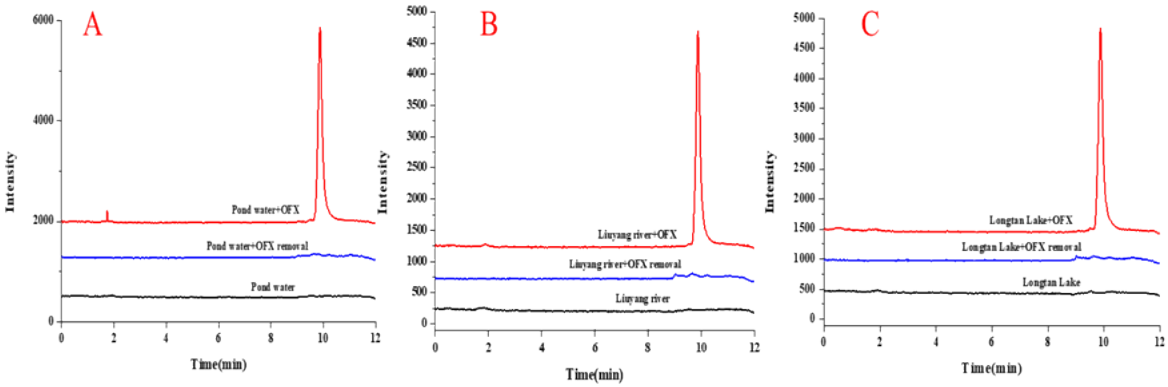

Figure S5 Typical chromatograms of pond water (A), rive water (B), and lake water (C) before and after degradation (20 min of light irradiation) via E-spun g-C_3N_4/$Bi_{12}O_{17}Cl_2$(1:3)/PANCMA nanofibers. The spiked OFL concentration was 100 ng/mL.

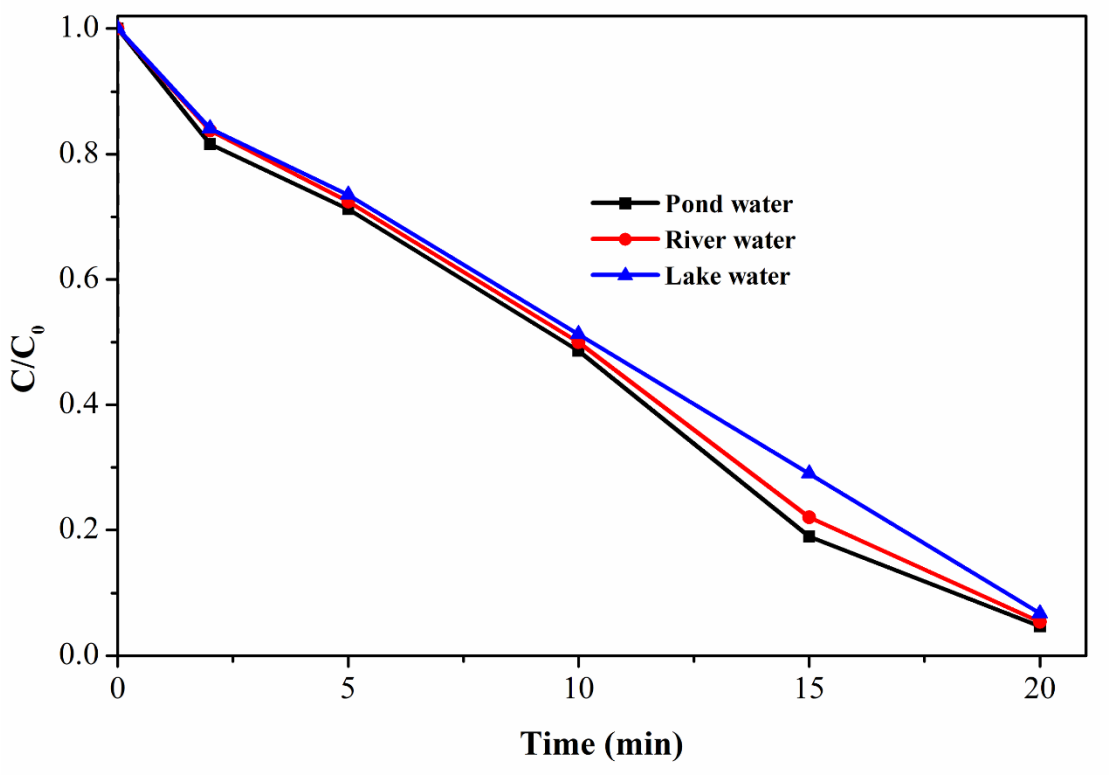

Figure S6 Photocatalytic degradation of OFL (50 mL, 100 ng/mL) in various water samples over E-spun g-C_3N_4/$Bi_{12}O_{17}Cl_2$(1:3)/PANCMA nanofibers

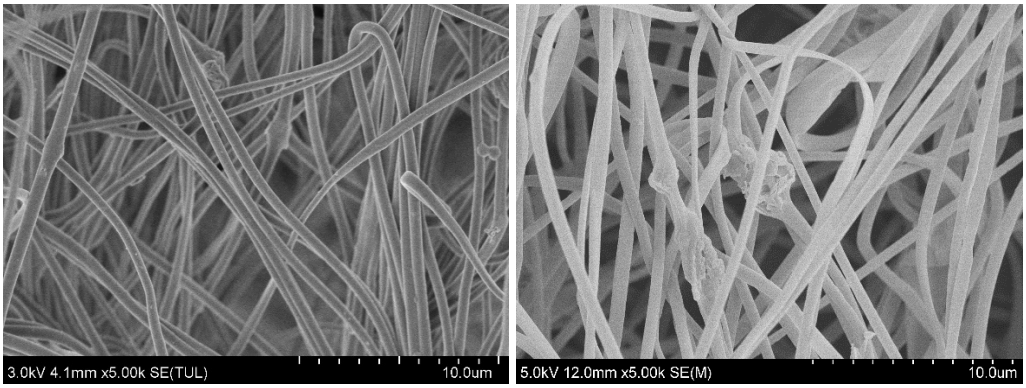

(A) (B)

Figure S7 SEM images of E-spun g-C_3N_4/$Bi_{12}O_{17}Cl_2$(1:3)/PANCMA nanofibers (A) before and (B) after consecutive 20 cycle times of adsorption/photocatalytic degradation process

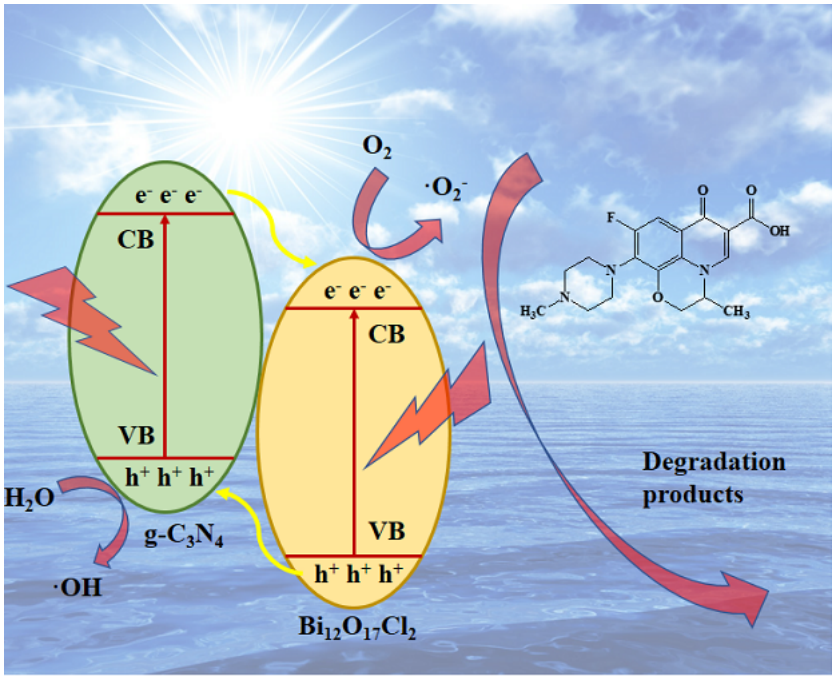

Scheme 1 Possible photocatalytic degradation mechanism of OFL over the E-spun g-C_3N_4/$Bi_{12}O_{17}Cl_2$(1:3)/PANCMA nanofibers